Study of Local Nonlinear Properties Using a Near-Field Microwave Microscope

Sheng-Chiang Lee and Steven M. Anlage, *Member, IEEE*

Abstract—We have developed a near-field microwave microscope to locally apply microwave frequency currents and fields to superconductors, and dielectric substrates, and measure the locally generated 2nd and 3rd harmonic responses. We measure the local nonlinear response of a $Tl_2Ba_2CaCu_2O_y$ film grown on an MgO substrate, and observe a large response due to the enhanced current density near the edge. We also study the local nonlinear response of a $YBa_2Cu_3O_{7-\delta}$ thin film grown on a bi-crystal $SrTiO_3$ (STO) substrate, and spatially identify the grain boundary through higher harmonic measurements. The spatial resolution is determined by the magnetic loop probe size. A scaling current density J_{NL} is extracted to quantify the magnitude of the nonlinearity of the superconductor. Preliminary results on the nonlinear properties of some commonly used substrates, e.g., MgO and STO, have also been obtained.

Index Terms—Harmonic generation, Josephson junctions, microwave measurements, microwave microscope, near-field, nonlinear, superconductivity.

I. INTRODUCTION

THE nonlinear properties of high-T_c superconductors have been of great concern in microwave applications due to their undesired intermodulation response at moderate power levels. While all superconductors have an intrinsic nonlinearity associated with the nonlinear Meissner effect, extrinsic nonlinearities due to topographic features, structural defects, and edge-current buildup are also inevitable in sample fabrication and applications. Several microscopic models, including BCS theory [1], [2], Ginzburg-Landau theory [3], and microwave field-induced modulation of the super/normal fluid density near T_c [4], have been proposed to understand the intrinsic nonlinearity of superconductors. However, upon comparing the expected intrinsic nonlinearity from these models with the extrinsic nonlinearity, the extrinsic nonlinear sources are seen to dominate the nonlinear behavior of many superconductors at most temperatures below T_c [5]. Many experiments have studied the nonlinearity of superconductors in terms of intermodulation distortion [5], [6], harmonic generation [7], [8], or the nonlinear surface impedance [9]–[11]. However, most of these experiments are done with resonant techniques, which by their nature study the averaged nonlinear response from the sample rather than locally, hence have difficulty in
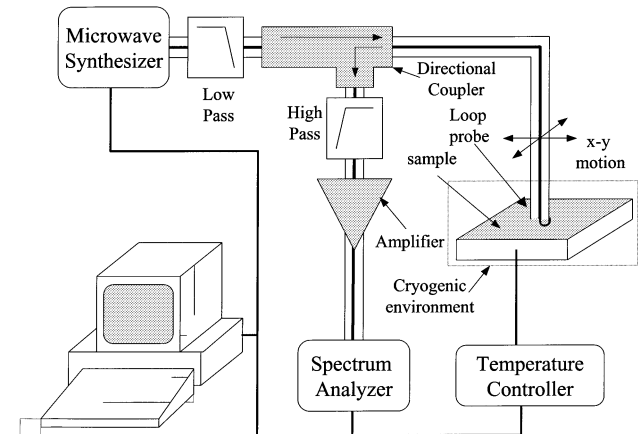
Fig. 1. Experimental setup. A synthesized tone at approximately 6.5 GHz is first low-pass filtered, and then sent to the tip of the microwave probe. There an rf current is induced in the sample, creating second and third-order nonlinear signals. These signals are gathered by the probe tip and high-pass filtered and amplified before being measured by the spectrum analyzer.

either avoiding edge effects, or determining the homogeneity, in terms of nonlinearities, of the sample. Therefore, a technique capable of locally measuring nonlinear properties of a sample is necessary for understanding the microscopic origins of superconducting nonlinearities.

II. EXPERIMENT AND DATA

A. Experimental Setup

In prior work [6], we studied the intermodulation signal from a high-T_c superconducting microwave resonator using a scanning electric field pick-up probe. Both the "global", and the "local" intermodulation power measured with the open-ended coaxial probe, were presented. However, the local measurements were actually a superposition of nonlinear responses that were generated locally but propagated throughout the microstrip and formed a resonant standing-wave pattern. To avoid this loss of local information, we have developed a nonresonant near-field microwave microscope, to nondestructively measure the local harmonic generation from un-patterned samples. This technique also works equally well through T_c and into the normal state of the sample. It also permits measurements with variable spatial resolution and rf current orientation. Finally, the experiment determines both the second and third harmonic nonlinearities at the same location, and does so at any frequency or temperature of interest.

In our experiment (Fig. 1), low pass filters are used to filter out higher harmonics generated by the microwave source, and
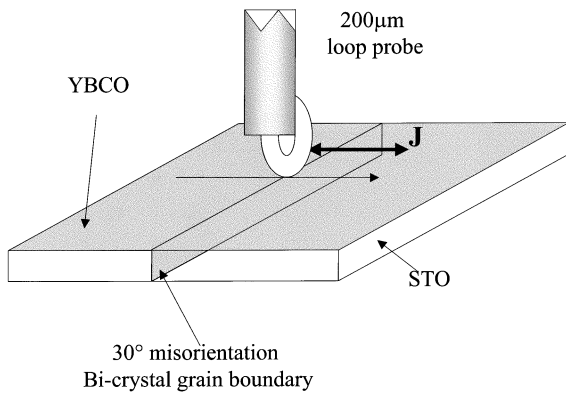
Fig. 2. The setup of a magnetic loop probe coupling to a YBCO/bi-crystal STO sample. The microwave current is determined by the loop orientation, which is put perpendicular to the 30° tilt mis-orientated YBCO grain boundary on the film.
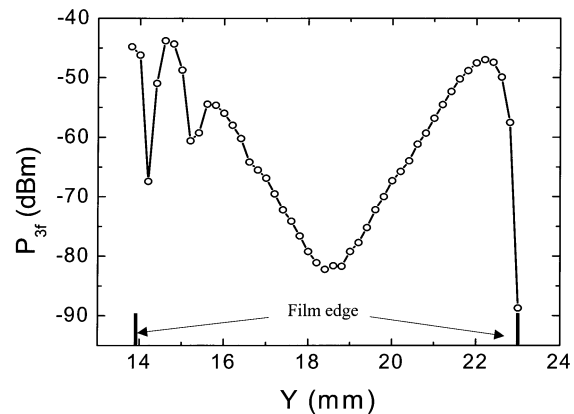

Fig. 3. Line cut of P_{3f} along the direction perpendicular to the induced microwave current on the TBCCO film taken at $T = 102.5$ K. A 6.5 GHz microwave signal of $+10$ dBm is applied to the sample. P_{3f} is enhanced tremendously upon approaching both edges, located at $\sim Y = 14$ mm, and 23 mm.
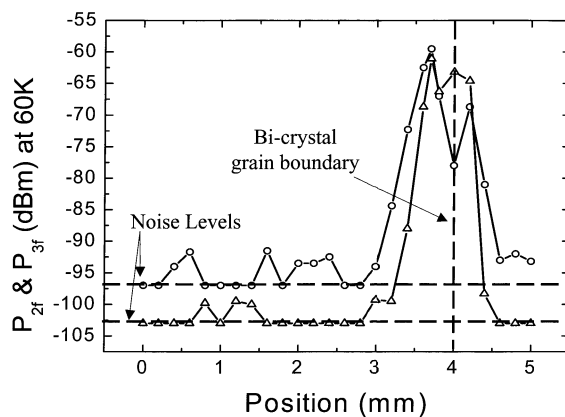

Fig. 4. Measurements of P_{2f} and P_{3f} versus position perpendicular to a YBCO bi-crystal GB at 60 K, while a $+8$ dBm, 6.5 GHz microwave signal is applied through a magnetic loop probe. The grain boundary is located near a position of 4 mm. Circles denote the 2nd and triangles denote the 3rd harmonic powers measured with a spectrum analyzer.

guarantee that only the selected fundamental frequency power P_f is sent to the sample, while the reflected harmonics are selected by 2 high pass filters, before being amplified by ~ 65 dB, and measured by a spectrum analyzer as P_{2f} and P_{3f}.

A loop probe, which is made of a coaxial cable with its inner conductor forming a semi-circular loop shorted with the outer conductor, [12] is designed to directionally enhance the magnetic coupling between the probe and sample, and induce microwave frequency currents of a controlled geometry in the sample (Fig. 2), while both the probe and the sample are kept in a high vacuum, cryogenic environment. The harmonic signals generated in the sample couple back to the loop probe to be filtered and measured by a spectrum analyzer. Since the probe can couple to the sample at points far away from the sample edge, the nonlinearity due to the edge-current buildup effect is eliminated. The probe can be translated over the surface of the sample in the x-y plane manually.

B. Sample

The superconducting samples we study are a ~ 5000 Å thick $Tl_2Ba_2CaCu_2O_y$ (TBCCO) film grown on a MgO substrate, and 500 Å thick $YBa_2Cu_3O_{7-\delta}$ (YBCO) thin films deposited by pulsed laser deposition on a bi-crystal STO substrate with a 30° tilt mis-orientation. The distance between the loop probe and the sample is fixed by a 12.5 μm thick Teflon sheet. The T_c of the TBCCO film is 105.6 K, as determined by 4-point zero resistance measurement, and the T_c of the plain YBCO and bi-crystal YBCO are 88.9 K and 88.8 K, respectively, as measured by ac susceptibility. Two commonly-used dielectric substrates, STO (5 mm $\times$ 5 mm $\times$ 0.5 mm) and MgO (10 mm $\times$ 10 mm $\times$ 1 mm), are also evaluated by this technique.

C. Data

Line-cut measurements of the 3rd order harmonic generation are performed on TBCCO using a magnetic loop probe at 102.5 K $< T_c$. While the probe is moved perpendicular to the uni-directionally induced current on the film, a clear increase in 3rd order nonlinear response is observed near the edge of the film, as shown in Fig. 3. The enhanced P_{3f} near the edge is due

to the large screening current at the edge required to prevent magnetic field, generated by the microwave current, from penetrating into the superconductor. All other measurements presented below take place in the middle of the film where the edge effects are not significant.

Measurements of the temperature dependent 2nd and 3rd order harmonic power (P_{2f} and P_{3f}) are performed on the YBCO bi-crystal film, both above the grain boundary (GB) and far away from the grain boundary (non-GB). A strong peak in $P_{3f}(T)$ near T_c is observed at both locations. [18] However, at temperatures far below T_c, $P_{2f}(T)$ and $P_{3f}(T)$ show strong temperature dependence above the GB, while they are not distinguishable from the noise in the non-GB areas. While Josephson vortices should be responsible for the observed P_{2f}, [13], [14] P_{3f} is due to the nonlinear impedance of the Josephson junction. [15]

Such a clear distinction between the response of GB and non-GB areas enables us to use this microscope to locally identify the bi-crystal grain boundary as a nonlinearity source in superconductors (Fig. 4). Here the probe is translated over the GB, which shows up as an enhanced nonlinear response.
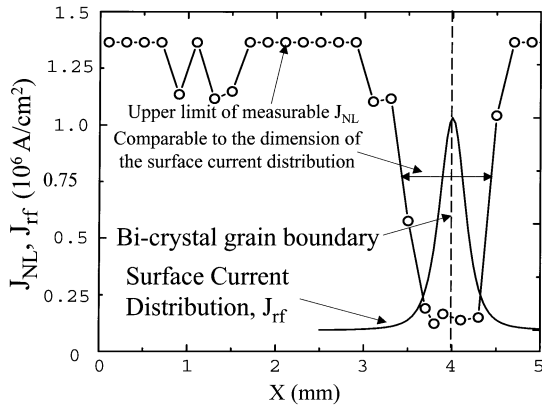
Fig. 5. The calculated nonlinear current scale, J_{NL}, from the P_{3f} data in Fig. 4. The upper limit corresponds to the noise level in our current setup, which is about -103 dBm. The curve plotted on the bottom is the calculated current density distribution beneath the probe, whose maximum is $\sim 10^6$ A/cm^2.

The spatial resolution is determined by the loop probe size, which is $\sim 500\ \mu$m in the experiment.

To further evaluate the capability of the microscope to detect superconducting nonlinearities due to different mechanisms, a scaling current density J_{NL} is extracted from the data in Fig. 4 based on the assumption of a leading-order quadratic dependence of the superfluid density on rf current density: $\lambda_L(T, J) \cong \lambda_L(T, 0)(1 + (J/J_{NL}(T))^2)^{1/2}$, where λ_L is the London penetration depth, and J_{NL} is the scaling current density, whose magnitude is determined by the nonlinearity mechanism. [5], [16]

We calculated numerically the current distribution on the superconducting film according to our experimental geometry, and use it to estimate the nonlinear inductance of the super-conductor. Following Booth's algorithm [16], the conversion between J_{NL} and measured P_{3f} is established. Fig. 5 shows the converted J_{NL} from the P_{3f} data in Fig. 4. The $J_{NL}(x)$ distribution shows a similar spatial resolution to both the P_{3f} and the probe surface current distribution. From the magnitude of the J_{NL} we extract ($\sim 1.5 \times 10^5$ A/cm^2), and its location, we confirm that the nonlinear response we observe is due to the bi-crystal grain boundary that forms a long Josephson junction along the boundary. Comparing the extracted J_{NL} with the critical current density J_c of YBCO bi-crystal junction at 30°, [17] we find that the J_{NL} is comparable to the $J_c \sim 10^4$–10^5 A/cm^2 of the YBCO junction. It is also worth noting that the J_{NL} extracted for the Josephson nonlinearity appears to be power dependent. This is because J_{NL} is calculated on the assumption of a quadratic power-law nonlinearity, and the Josephson nonlinearity is generally not a quadratic power-law [5]. Nevertheless, the calculation of J_{NL} still gives a quantitative understanding of the magnitudes of different nonlinear sources.

The sensitivity of our current setup is limited to $J_{NL} \leq 1.3 \times 10^6$ A/cm^2. Since the magnitudes of the measured nonlinear responses are determined by the loop-sample coupling, enhancing this coupling will increase our sensitivity to J_{NL}. This can be done by reducing the size of the probe, so that the effective distance between the probe and sample is reduced, and the coupling enhanced. Our calculations also suggests
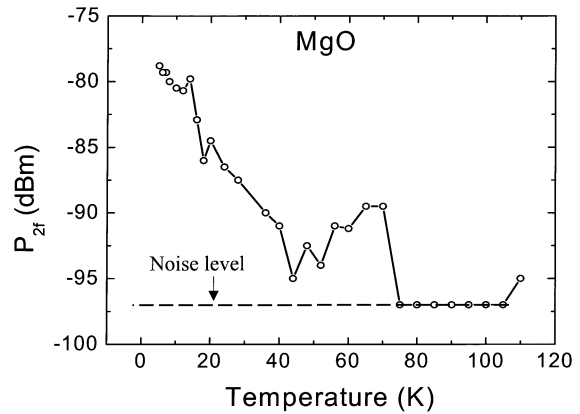

Fig. 6. Temperature dependence of P_{2f} of an MgO substrate, measured by a magnetic loop probe with a primary tone at 6.5 GHz.
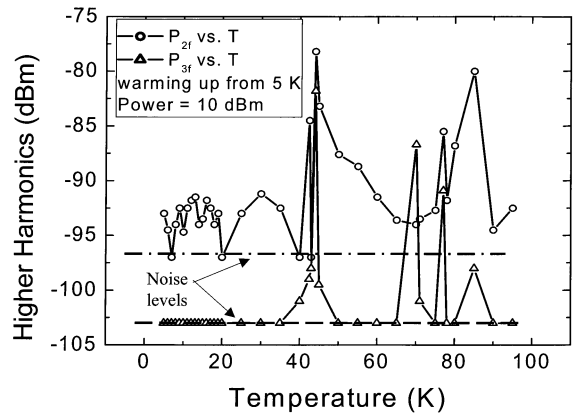

Fig. 7. Temperature dependent $P_{2f}(T)$ and $P_{3f}(T)$ of STO, measured by a magnetic loop probe with a primary tone at 6.5 GHz. The dashed and dot-dashed lines are the noise levels for P_{2f} (upper) and P_{3f} (lower) measurements, respectively.

that as long as the film thickness is less than the penetration depth, thinner films will generate stronger nonlinear responses from the same nonlinear source (same J_{NL}) while applying microwaves of the same power. More discussion of our work on this YBCO bi-crystal grain boundary with Josephson junction model and J_{NL} can be found in [18].

It has recently become clear that the dielectric substrates used in high temperature superconducting microwave devices are also nonlinear [19], [20]. Therefore, similar experiments of 2nd and 3rd harmonic generation were performed on bare MgO and STO substrates using the magnetic loop probe.

A clear temperature-dependent $P_{2f}(T)$ is observed on MgO (Fig. 6), while $P_{3f}(T)$ is not detectable above the noise with the loop probe between 4 K and 110 K. A defect dipole relaxation model has been suggested to interpret the measured nonlinear properties of MgO. [18] The second harmonic signal we see here is consistent with the Fe-impurity mechanism proposed as the source of nonlinearity in MgO [18]. Our experiment may provide another approach to study the nonlinear response of MgO, although the data is preliminary at this moment.

Temperature dependent $P_{2f}(T)$ and $P_{3f}(T)$ are also observed on a STO substrate, within narrow temperature windows at certain temperatures (Fig. 7). We believe this is due to its strongly temperature-dependent dielectric constant, so that

when a fixed-frequency microwave signal is applied, the substrate becomes a microwave dielectric resonator at temperatures corresponding to the appropriate dielectric constants. The enhanced P_{2f} and P_{3f} may be due in part to resonantly-enhanced background nonlinearity signals.

III. CONCLUSION

We have shown that our near-field microwave microscope is capable of identifying local nonlinear sources, such as a bi-crystal grain boundary and edge-effects, with a spatial resolution similar to the loop probe size. By reducing the loop probe size, the spatial resolution can be further improved. We are also able to convert the measured P_{3f} to a scaling current density J_{NL}, which provides a common ground to quantitatively compare the magnitudes of different nonlinearities. The sensitivity of our microscope to J_{NL} can be improved by reducing the probe size and the film thickness. On the other hand, our preliminary work on nonlinear dielectrics, such as MgO and STO, also shows the capability of using this microscope to locally characterize nonlinear dielectric substrates, which is helpful in evaluating the impact of such substrates in microwave applications of superconducting devices.

REFERENCES

[1] S. K. Yip and J. A. Sauls, "Nonlinear Meissner effect in CuO superconductors," *Phys. Rev. Lett.*, vol. 69, pp. 2264–2267, 1992.
[2] T. Dahm and D. J. Scalapino, "Theory of intermodulation in a superconducting microstrip resonator," *J. Appl. Phys.*, vol. 81, pp. 2002–2009, 1997.
[3] J. Gittleman, B. Rosenblum, T. E. Seidel, and A. W. Wicklund, "Nonlinear reactance of superconducting films," *Phys. Rev.*, vol. 137, pp. A527–A536, 1965.
[4] I. Ciccarello, C. Fazio, M. Guccione, and M. Li Vigni, "Nonlinear magnetization of YBCO single crystal near T_c," *Phys. Rev. B*, vol. 49, pp. 6280–6284, 1994.
[5] B. A. Willemsen, K. E. Kihlstrom, T. Dahm, D. J. Scalapino, B. Gowe, D. A. Bonn, and W. N. Hardy, "Microwave loss and intermodulation in TBCCO thin films," *Phys. Rev. B*, vol. 58, pp. 6650–6654, 1998.
[6] W. Hu, A. S. Thanawalla, B. J. Feenstra, F. C. Wellstood, and S. M. Anlage, "Imaging of microwave intermodulation fields in a superconducting microstrip resonator," *Appl. Phys. Lett.*, vol. 75, pp. 2824–2826, 1999.
[7] C. Wilker, Z.-Y. S. P. Pang, W. L. Holstein, and D. W. Face, "Nonlinear effect in high temperature superconductors: 3rd order intercept from harmonic generation," *IEEE Trans. Appl. Supercond.*, vol. 5, pp. 1665–1670, 1995.
[8] E. E. Pestov, Y. N. Nozdrin, and V. V. Kurin, "Third-order local nonlinear microwave response of YBCO and Nb thin films," *IEEE Trans. Appl. Supercond.*, vol. 11, pp. 131–134, 2001.
[9] P. P. Nguyen, D. E. Oates, G. Dresselhaus, and M. S. Dresselhaus, "Nonlinear surface impedance for YBCO thin films: Measurements and a coupled-grain model," *Phys. Rev. B*, vol. 48, pp. 6400–6412, 1993.
[10] D. E. Oates, Y. M. Habib, C. J. Lehner, L. R. Vale, R. H. Ono, G. Dresselhaus, and M. S. Dresselhaus, "Measurement and modeling of microwave impedance of high-T_c grain boundaries," *IEEE Trans. Appl. Supercond.*, vol. 9, pp. 2446–2451, 1999.
[11] I. Ciccarello, C. Fazio, M. Guzzione, and M. Li Vigni, "Complex conductivity in high-T_c single crystal superconductors," *Ann. Physik*, vol. 3, pp. 13–20, 1994.
[12] S. C. Lee, C. P. Vlahacos, B. J. Feenstra, A. Schwartz, D. E. Steinhauer, F. C. Wellstood, and S. M. Anlage, "Magnetic permeability imaging of metals with a scanning near-field microwave microscope," *Appl. Phys. Lett.*, vol. 77, pp. 4404–4406, 2000.
[13] Y. M. Habib, C. J. Lehner, D. E. Oates, L. R. Vale, R. H. Ono, G. Dresselhaus, and M. S. Dresselhaus, "Measurements and modeling of the microwave impedance in high-T_c grain-boundary Josephson junctions: Fluxon generation and rf Josephson-vortex dynamics," *Phys. Rev. B*, vol. 57, pp. 13 833–13 844, 1998.
[14] C. J. Lenher, D. E. Oates, Y. M. Habib, G. Dresselhaus, and M. S. Dresselhaus, "Modeling the microwave impedance of high-T_c long Josephson junction," *J. Supercond.*, vol. 12, pp. 363–375, 1999.
[15] J. McDonald and J. R. Clem, "Microwave response and surface impedance of weak links," *Phys. Rev. B*, vol. 56, pp. 14 723–14 732, 1997.
[16] J. C. Booth, J. A. Beall, D. A. Rudman, L. R. Vale, and R. H. Ono, "Geometry dependence of nonlinear effects in high temperature superconducting transmission lines at microwave frequencies," *J. Appl. Phys.*, vol. 86, pp. 1020–1027, 1999.
[17] H. Hilgenkamp and J. Mannhart, "Grain boundaries in high-T_c superconductors," *Rev. Mod. Phys.*, vol. 74, pp. 485–549, 2002.
[18] S. C. Lee and S. M. Anlage, "Spatially resolved nonlilnearity measurements of YBa$_2$Cu$_3$O$_{7-\delta}$ bi-crystal grain boundaries," Appl. Phys. Lett., 2002, submitted for publication.
[19] M. A. Hein, D. E. Oates, P. J. Hirst, R. G. Humphreys, and A. V. Velichko, "Nonlinear dielectric microwave losses in MgO substrates," *Appl. Phys. Lett.*, vol. 80, pp. 1007–1009, 2002.
[20] E. I. Golovenchits, V. A. Sanina, and A. V. Babinskii, "Nonlinear dielectric susceptibility in STO and possible nature of the low-temperature phase," *JETP Lett.*, vol. 63, no. 8, pp. 674–679, 1996.